The Importance of Heat Conduction and Viscosity in Solar Corona and Comparison of Magnetohydrodynamic Equations of One-Fluid and Two-Fluid Structure in Current Sheet

Umit Deniz Goker

Astronomy and Space Sciences Department, Science Faculty, Ege University, Izmir, Turkey

e-mail: udenizg@gmail.com

Received: 15 October 2008; Accepted: 29 December 2008

Abstract. Magnetic reconnection (MR) plays an important role in solar flares, coronal heating and geomagnetic substorms. A number of magnetohydrodynamic (MHD) discontinuities can be produced by MR. Previous studies showed that the heat conductivity parallel to the magnetic field was much larger than the perpendicular conductivity. On the other hand recent SOHO observations have shown that perpendicular heat conductivity plays an important role in an MR region. In this paper numerical simulations that take into account the effects of both parallel and perpendicular heat conductivities are presented. When the viscosity parameter was added, real shock formation under jump conditions was not observed. While temperature is increasing smoothly, a cut-off shape in initial and final limits of the shock wave was calculated for density and pressure. In this paper a comprehensive simulation of the one-fluid structure is presented. Extension of this work to simulations of two-fluid structure is proposed.

Keywords: shock waves; current sheet; heat conduction; viscosity

1. Introduction

Viscosity and heat conduction are two important effects for magnetohydrodynamic (MHD) waves. While the ions contribute significantly to the viscosity, much of the heat conduction is due to electrons. The temperature and pressure in the inflow region of magnetic reconnection (MR) are significantly modified by the heat conduction. Non-linear instability is largely determined by the balance between parallel and perpendicular heat transport [1].

The dissipative mechanism (entropy and heat conduction) controls only the values of the gradients of the flow variables in the transition layer but doesn't affect the jumps in these quantities between the initial and the final stages. These changes are determined solely by the conservation laws [2]. In this work we use the typical values for the solar corona: $L = 5 \times 10^6$ m (the length of the solar corona), $B = 10^{-3}$ T (the magnetic field), $n = 2 \times 10^{15}$ m^{-3} (the density of electrons), $\ln \Lambda = 20$ (Coulomb logarithm) and the temperature is $T_e = T_i = T =$ 172 eV. We assumed one-fluid structure for the heat conduction and viscosity parameters of the electrons.

In section 2 the theoretical and mathematical frame of work is presented. In sections 3 and 4 a detailed numerical simulation is presented for one-fluid structure. Section 5 describes the possible extension of the one-fluid structure to two-fluid structure. Section 6 discusses the implication of the simulation and its potential application for two-fluid structure. In section 7 the results of the simulation for one-fluid structure are presented.

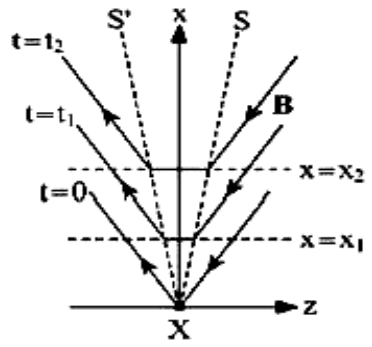

Fig. 1. The formation of slow shocks in the outflow region of magnetic recconnection in the X-Z plane. The initial current sheet is located in the plane z = 0. The orientation of the current sheet is in the x-direction. The magnetic field line reconnected at t = 0 is convected to x_1 and x_2 at time t_1 and t_2, respectively. For t > 0, a pair of slow shocks propagate in the $\pm$ z direction. Two slow shocks XS and XS' emanate from the point X [3].

2. General conservative equations for one-fluid structure in the current sheet

The slow shocks in the outflow region of MR consist of two parts: *the isothermal main shock* and *foreshock*. Significant jumps in plasma density, velocity and magnetic field occur across the main shock. The foreshock is featured by a smooth temperature variation

and is formed due to the heat flow from downstream to upstream regions [3]. The slow shocks are formed along *XS´* and *XS* in the upper X-Z plane (Fig. 1). For $t > 0$, a pair of slow shocks is formed through the evolution of a current sheet initiated by the presence of a normal magnetic field.

The MHD equations for shock waves in the current sheet are defined below and we have added a viscosity term to the momentum and energy equations. For the first time the perpendicular heat conduction is included into the heat conduction term in the energy equation (Eq. (4)). Since shock waves are governed by the jump conditions, the MHD equations were formed followed by the evaluation and simulation of the jump conditions for one fluid structure.

$$\frac{\partial \rho}{\partial t} = -\nabla.(\rho \mathbf{V}) \tag{1}$$

$$\frac{\partial(\rho \mathbf{V})}{\partial t} = -\nabla.\left[\rho \mathbf{V}\mathbf{V} + \left(P + \frac{B^2}{8\pi}\right)\hat{\mathbf{I}} - \frac{1}{4\pi}\mathbf{B}\mathbf{B} + \omega_{jk}\right] \tag{2}$$

$$\frac{\partial \mathbf{B}}{\partial t} = \nabla \times (\mathbf{V} \times \mathbf{B}) \tag{3}$$

$$\frac{\partial}{\partial t}\left(\frac{\rho V^2}{2} + \frac{P}{\gamma - 1} + \frac{B^2}{8\pi}\right) = -\nabla.\left[\left(\frac{\rho V^2}{2} + \frac{\gamma P}{\gamma - 1} + \omega_{jk}\right)\mathbf{V} - \frac{1}{4\pi}(\mathbf{V} \times \mathbf{B}) \times \mathbf{B}\right] + \nabla.(\mathbf{K}.\nabla T) \tag{4}$$

This set of MHD equations (1-4) constitutes the mass continuity, momentum equation, magnetic induction and energy equation, respectively. In these equations ρ, P, **V** and **B** indicates the mass density, pressure, flow velocity and the magnetic field, respectively. In Eqs. (2) and (4), ω_{jk} represents the "*viscosity tensor*" and $\hat{\mathbf{I}}$ is a unit vector [4].

$\mathbf{V_t} = (V_x, V_y)$ and $\mathbf{B_t} = (B_x, B_y)$, where V_x, V_y and B_x, B_y are transverse components of the velocity and magnetic field, respectively. The ion and electron temperature profiles are equal, i.e. $T_i \cong T_e \cong T$. On the right hand side of the energy equation, $\nabla.(\mathbf{K}.\nabla(kT_e)) = \nabla.(-\mathbf{q})$ describes heat flux term, where, **K** is the thermal conduction tensor. Following [5], $\mathbf{K} = \mathrm{K}_{//}\mathbf{bb} + \mathrm{K}_{\perp}(\hat{\mathbf{I}} - \mathbf{bb})$, where $K_{//}$ and $K_{\perp}$ are, the parallel and perpendicular coefficients of the electron thermal conductivity, respectively; and **b** = **B**/B. The values of $K_{//}$ and $K_{\perp}$ were extracted from [6]. In the energy equation,

$$\varepsilon = \left(\frac{\rho V^2}{2} + \frac{P}{\gamma - 1} + \frac{B^2}{8\pi}\right)$$

is the internal energy.

3. Numerical simulation

The numerical simulation was performed using Lagrangian Remap Code (Lare Xd) [7]. In this code the MHD equations are in Lagrangian form. All grid points move with local flow speed. Remap steps do not include physics; it gives the results in a mathematical form. The constants in the code are the width of initial current sheet (δ = 0.025), the upstream shock angle ($\theta_1 = \pi/4$), the plasma beta (β = 0.04) and the adiabatic index (γ= 5/3).

TABLE 1
Assumptions in the Numerical Code

Assumptions	Parameters
Initial Conditions	$V_{x0} = V_{z0} = 0$ B_z = constant T (temperature) = constant $\mathbf{B}(z) = -B_\infty \sin\theta_1 \tan(z/\delta)\,\hat{x} + B_\infty \cos\theta_1\,\hat{z}$ $P = \beta.B^2 / 2 = \beta.\left(B_x^2 + B_z^2\right) / 2$
Boundary Conditions	For $z = 1$, $\partial V_x / \partial z = \partial V_z / \partial z = 0$ For $z = 0$, $\partial B_x / \partial z = V_z = 0$ Along $z = 0$, **E** = 0

In the Remap step, the conduction equation is $\nabla.B = 0.$ The numerical code identified in Table 1 is assumed. The advantage of this code is that it calculates automatically the continuity of mass, momentum and thermal energy. It can easily capture the shocks, calculate the local temperature, and other non-hyperbolic physical values such as resistivity, viscosity, radiation, thermal conduction, gravity, etc.

At t=0 the velocity doesn't change therefore V_{x0}=V_{Z0}=0 and the magnetic field, B_z=0 along the direction of the shock. B_z remains constant during the shock formation. Moreover **B**(z) is the profile of the magnetic field and B_∞ denotes the magnetic field far from the current sheet. A pair of slow shocks propagating in the ± z direction leads to a negative x-component of the magnetic field. This is possible because the magnetic field perpendicular to the direction of propagation of the shock changes in both positive and negative directions. Both the pressure (P) and the density (ρ) are proportional to the magnetic field.

At the boundary, for z = 0, where the initial current sheet is located at the center of simulation domain, the parallel component of the initial velocity and the spatial derivative of the magnetic field in the perpendicular direction will be zero. Along z = 0, total electric field assumes **E** = 0. There is no electrical dependence (or conductivity) at one-fluid structure. For z = 1, where the final stage of the current sheet is located at the final simulation domain, the spatial derivatives of the velocity along the parallel and perpendicular direction can not be observed.

4. Jump conditions and the first results

Since the integrals on the left-hand side of the Eqs.(1-4) are proportional to $z_2 - z_1$, in steady-state limit they vanish. Here z_1 , z_2 define the region before and after the shock, respectively. This is because the thickness of the shock layer $z_2 - z_1$ goes to zero. This corresponds to the absence of mass, momentum and energy accumulation in the discontinuity. On the other hand the integrals on the right hand side give the difference between the

various fluxes on each side of the discontinuity heralding the jump conditions [1]:

$$\left[\rho V_z\right] = 0 \tag{5}$$

$$\left[\rho V_z^2 + P + \frac{B^2}{2} + 2\times10^{-15} T^{5/2}\left(\frac{\partial V_z}{\partial z}\right)\right] = 0 \tag{6}$$

$$\left[\rho V_z \mathbf{V}_t - B_z \mathbf{B}_t + 8\times10^{-17} B^{-2} T^{-1/2}\left[\frac{\partial V_x}{\partial z}\mathbf{i} + \frac{\partial V_y}{\partial z}\mathbf{j}\right]\right] = 0 \tag{7}$$

$$\left[V_z \mathbf{B}_t - B_z \mathbf{V}_t\right] = 0 \tag{8}$$

$$\left(\left(\varepsilon + P + \frac{B^2}{2}\right)V_z - (\mathbf{V}.\mathbf{B})B_z + \left[8.3\times10^{12} T^{5/2}\left(\frac{B_z}{B}\right)^2 \frac{\partial(k_B T)}{\partial z} + 1.7\times10^{11} B^{-2} T^{-1/2}\left[\frac{\partial(k_B T)}{\partial z} - \left(\frac{B_z}{B}\right)^2 \frac{\partial(k_B T)}{\partial z}\right]\right] + 8\times10^{-17} B^{-2} T^{-1/2}\left[V_x \frac{\partial V_x}{\partial z} + V_y \frac{\partial V_y}{\partial z}\right]\right) = 0 \tag{9}$$

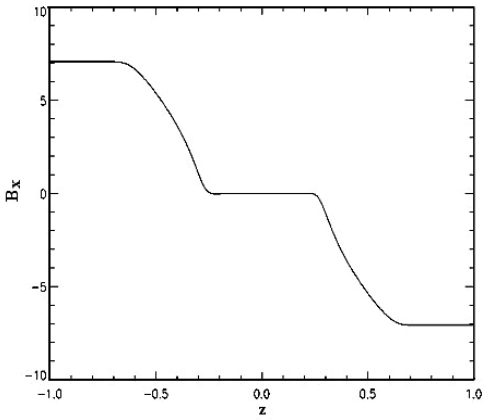

Fig. 2. Spatial profile of B_x (perpendicular magnetic field) at t = 200.

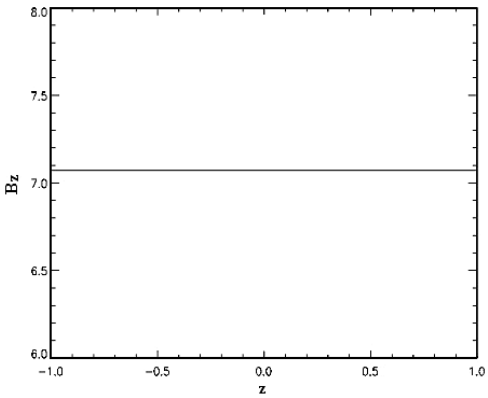

Fig. 3. Spatial profile of B_z (parallel magnetic field) at t = 200.

The spatial derivative of the magnetic field in the direction of shock propagation does not change because there is no jump in the parallel magnetic field and B_z remains constant. It can be seen in the Fig.3.

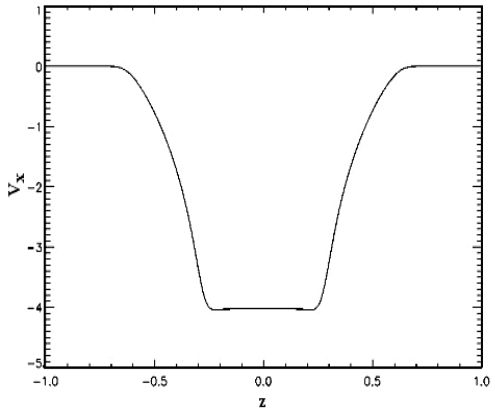

Fig. 4. Spatial profile of V_x (perpendicular velocity) at t = 200.

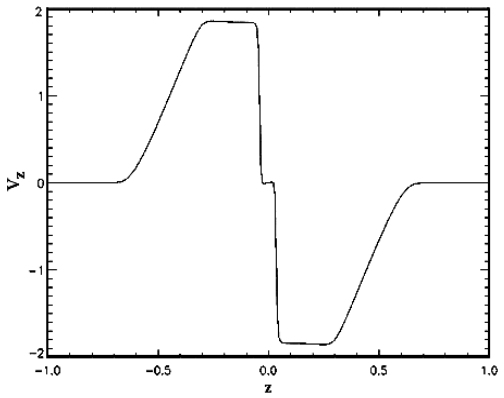

Fig. 5. Spatial profile of V_z (parallel velocity) at t = 200.

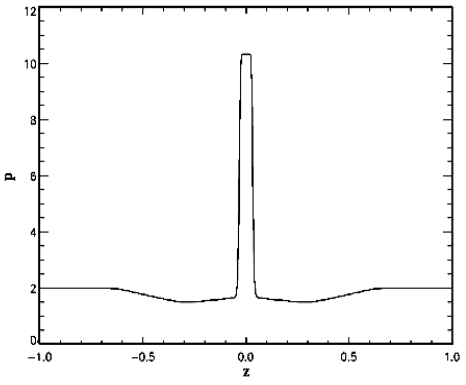

Fig.6. Spatial profile of pressure at t = 200.

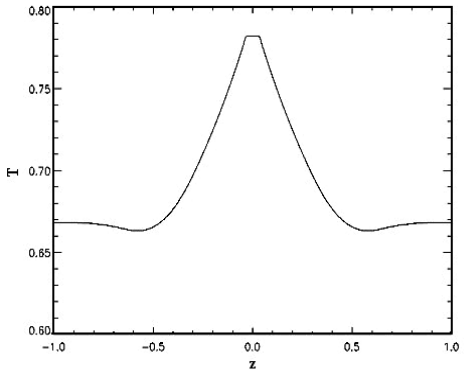

Fig.7. Spatial profile of temperature at t = 200.

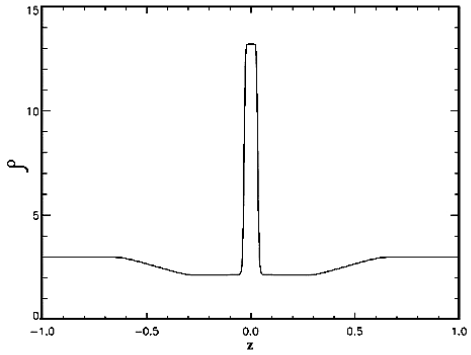

Fig. 8. Spatial profile of density at t = 200.

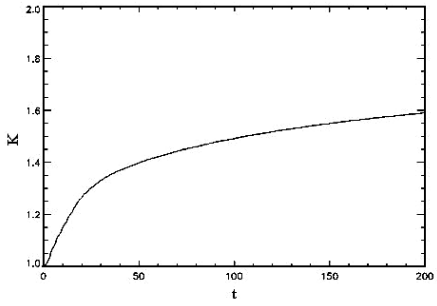

Fig. 9. The variation of K as a function of time.

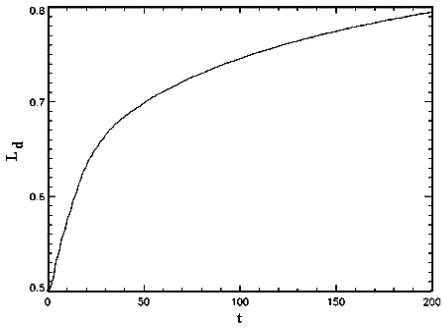

Fig. 10. The variation of L_d as a function of time.

During the shock the temperature is conservative, i.e. [T]=0. The simulation time was 200 sec. As shown in Figures (2-8) the jump conditions at z = 0 are observed in the current sheet. Figs.9 and 10 are the time variations of *K* (the heat conductivity) and L_d (the foreshock width).

For isotropic plasma (γ=5/3) and using the respective jump conditions the general equation was obtained. We combine Eqs.(5-8) together and accommodate them into the energy equation Eq.(9) to obtain the general equation below:

$$r^3\left[5\beta_1\cos^4\Theta_1+2M_{A1}^2\cos^2\Theta_1\right]+r^2\left[-10\beta_1M_{A1}^2\cos^2\Theta_1 - 5M_{A1}^4\cos^2\Theta_1+M_{A1}^4-8M_{A1}^2\cos^2\Theta_1\right] + r\left[5\beta_1M_{A1}^4+2M_{A1}^6+11M_{A1}^4\cos^2\Theta_1+5M_{A1}^4\right] - 8M_{A1}^6=0 \quad (10)$$

Here, $r=\rho_2/\rho_1$, $\beta_1=P_1/\left(B_1^2/2\right)=2C_{S1}^2/\gamma V_{A1}^2$ and $M_{A1}=V_{z1}/V_{A1}=V_{z1}\rho_1^{1/2}/B_1$, where C_{s1} is a sound wave's velocity, M_{A1} is the Mach number and V_{A1} is the Alfven velocity in the upstream region.

5. Extention of one-fluid structure model to two-fluid structure

The current sheet is an essentially two-temperature medium ($T_e \neq T_i$) and is associated with almost a collisionless plazma. In spite of this, collisional dissipative effects in MHD equations are important for two-fluid structure. Extension to two-fluid MHD equations from one-fluid equations followed two steps: **Step 1**: add Ohm's law and a fluid friction element to the momentum and energy equation, and, **Step 2**: add to the energy equation the heat transfer term due to collisions.

For two-fluid structure, the "*total plasma mass density*" $\rho_{tot}\equiv m_en_e+m_in_i$ and the pressure will be the "*total thermal pressure*": $P_{tot}=n_ek_BT_e+n_ik_BT_i$. For a quasi-neutral plasma ($n_e=Zn_i$) and ion charge number *Z* = 1 (Hydrogen), the total number density becomes $n=3.6\times10^{16}\ m^{-3}$; and $\mu=m_i/m_p$. Under these conditions the modified one-fluid structure yields the following equations:

$$\frac{\partial\rho_\beta}{\partial t}=-\nabla.\left(\rho_\beta\mathbf{V}_\beta\right)\ ,\ \beta=e,i \quad (11)$$

$$\frac{\partial\left(\rho_\beta\mathbf{V}_\beta\right)}{\partial t}=-\nabla.\left[\rho_\beta\mathbf{V}_\beta\mathbf{V}_\beta+\left(P_\beta+\frac{B^2}{8\pi}\right)\hat{\mathbf{I}}-\frac{1}{4\pi}\mathbf{BB}+\Pi_{jk}^\beta\right] - q_\beta n_\beta\left(\mathbf{E}+\mathbf{V}_\beta\times\mathbf{B}\right)+\mathbf{R}_\beta \quad (12)$$

$$\frac{\partial\mathbf{B}}{\partial t}=\nabla\times\left(\mathbf{V}_\beta\times\mathbf{B}\right)+\eta\nabla^2\mathbf{B} \quad (13)$$

$$\frac{\partial}{\partial t}\left(\frac{\rho_\beta V_\beta^2}{2}+\frac{P_\beta}{\gamma-1}+\frac{B^2}{8\pi}\right)=-\nabla.\left[\left(\frac{\rho_\beta V_\beta^2}{2}+\frac{\gamma P_\beta}{\gamma-1}+\Pi_{jk}^\beta\right)\mathbf{V}_\beta - \frac{1}{4\pi}\left(\mathbf{V}_\beta\times\mathbf{B}\right)\times\mathbf{B}\right]+\nabla.\left(\mathbf{K}.\nabla T_\beta\right)+q_\beta n_\beta\mathbf{V}_\beta.\mathbf{E} + \mathbf{V}_\beta.\mathbf{R}_\beta+Q_\beta \quad (14)$$

When **E** = 0 at the current sheet, the current density becomes $\mathbf{j} = \sigma(\mathbf{V} \times \mathbf{B})$. Hence, the total magnetic field in Eq.(12) becomes positive for ions.

$R_e = -R_i = -\alpha_0 n_e q_\beta \left[\hat{\mathbf{b}} \left(\frac{J_{//}}{\sigma_{//}} \right) + \frac{J_\perp}{\sigma_\perp} \right]$ is the friction of the electron fluid element [8-9]; here α_0 is a dimensionless parameter is a function of *Z* of the ion. For, *Z* = 1 $\alpha_0 = 0.5129$ and *Z* = 2, $\alpha_0 = 0.4408$. $q_e = -e$ and $q_i = Z_i e$; $\sigma_{//} = 1.96 \frac{ne^2 \tau_e}{m_e}$ and $\sigma_\perp = 0.51 \sigma_{//}$ (σ is the electricalconductivity of the plasma).

$$Q_i = \frac{3 m_e n_e}{m_i \tau_e} (T_e - T_i)$$

and

$$Q_e = -R_e (\mathbf{V}_e - \mathbf{V}_i) - Q_i$$

are the heat transfer due to elastic collisions between the electrons and the ions [8-9]. η is the magnetic diffusivity coefficient.

6. Discussion

In this paper a comparison is made between one-fluid and two-fluid structure of the MHD equations. When dissipative effects such as Ohm's law, fluid friction element and heat transfer term are added the simulation of two-fluid structure will show significant deterioration of the shock waves profiles. It is not possible to see the discontinuity clearly in the two-fluid structure as compared to one-fluid profiles. Instead the shock profiles become continuous. Calculating the numerical simulation of two-fluid structure is not easy and more work is needed. This work has shown the possible evolution of the MHD equations from one-fluid structure to two-fluid structure. The next logical step to future work would be to comparison of the simulations and characterize the MR region.

In collisionless plasma, ions resonate with the cyclotron driver and attain high perpendicular velocities Protons and other ions have high perpendicular temperatures compared to their parallel temperatures $T_\perp >> T_{//}$ [2]. Viscosity in the jump conditions prevents real shock formation. In the solar corona, the *bulk or kinematic* viscosity value will be important because it consists of compressibility and it depends on the divergence of velocity effects of the formation of slow shocks [1].

The mistakes and defects in the code is that B_∞ = 20, energy and temperature variation will not be smooth and shock perturbations of initial and final stages need improving. For background viscosities, the values of density and pressure produce a shock wave which has a concave curve. Temperature, *K* and L_d profiles are good when the Braginskii viscosity were used without the other background viscosity parameters such as shock linear viscosity and shock quadratic viscosity.

7. Conclusions

The structure of slow shock in the presence of heat conduction both parallel and perpendicular to the magnetic field with viscosity coefficient was simulated with Lare Xd code. For the first time the perpendicular heat conduction in one-fluid structure used and the effect of viscosity also added. The dissipative effects give very interesting results. First, the real shock structure can't be observed when these effects were added. As shown in Figs. 6 and 8, the pressure and the density have showed a "cut-off shape" in initial and final limits of the shock wave because of the viscosity parameter. When viscosity make the slumps at the edges, the perpendicular heat conductivity produces narrow shock formation in the temperature profile. As shown in Fig. 7, the temperature increases smoothly from downstream to initial upstream value across the foreshock. Depending on the perpendicular heat conduction and viscosity term, the pressure and the density downstream of the main shock decreases with time very sharply as seen in Figs. 6 and 8.

The thermal conduction value *K* in the foreshock is proportional to time. Similarly the width of L_d in the foreshock increases linearly with time. The downstream temperature increases with time, while the downstream density in the main shock decreases with time. Since the thermal conductivity *K* is proportional to $T^{5/2}$, the diffusion width $L_d \sim \sqrt{Kt}$ is expected to increase with β_∞.

In Fig.2, B_x shows perpendicular variation of the magnetic field. The magnetic field begins decreasing after the shock at z = 0 point. This effect can also be seen for parallel velocity as shown in Fig.5 in the upstream region. Fig.4 shows that the perpendicular velocity increases linearly with shock propagation while the parallel velocity is decreasing with time.

Acknowledgements

The author wishes to thank Prof. Graham Hall and Serhan Yigen for their valuable comments and discussions.

REFERENCES

[1] Ya.B.Zel'dovich, Yu.P.Raizer, , "Physics of Shock Waves and High-Temperature Hydrodynamic Phenomena", Academic Press, 1966, 464 pages.

[2] M.A.Liberman, A.L.Velikovich, "Physics of Shock Waves in Gases and Plasmas", Springer-Verlag, (Springer Series in Electrophysics. v. 19), 1986, 396 pages.

[3] C.L.Tsai, R.H.Tsai, B.H.Wu, L.C.Lee, "Structure of slow shocks in a magnetized plasma with heat conduction", Physics of Plasmas, 2002, v. 9, n. 4. pp. 1185-1191.

[4] S.R.Seshandri, "Fundamental of Plasma Physics", American Elsevier Pub. Co., Inc., NY, 1973, 560 pages.

[5] S.I.Braginskii, "Transport Processes in a Plasma", in: Reviews of Plasma Physics, ed. M.A. Leontovich (Consultants Bureau, New York, 1965), 1965, v.1, pp. 205-311.

[6] J.D.Huba, "NRL Plasma Formulary", Beam Physics Branch, Plasma Physics Division, Naval Research Laboratory, Washington, DC 20375, 2002, 65 p.

[7] T.Arber, C.Brady, M.Haynes, , "Lare Xd User Guide", Centre for Fusion, Space and Astrophysics, University of Warwick, 2007, 29 p.

[8] Hu.Yemin, Hu.Xiwei, "The Properties and Structure of Plasma Non-neutral Shock", Physics of Plasmas, 2003, v. 10, v. 7, pp. 2704-2711.

[9] J.D.Callen, "Fundamentals of Plasma Physics", Lecture Notes, University of Wisconsin, Madison, 2003, 335 p.